Micromagnetic Tomography in Practice

Master Thesis

Annemarieke Béguin 3673006
Supervisor Lennart de Groot
Utrecht University
2016

Content

Abstract

Methods to derive paleodirections or paleointensities from rocks currently rely on measurements of bulk samples (typically ~10 cc), the obtained magnetization is a result of the sum of the magnetization from all the differing grains within the sample. The process of recording and storing magnetizations as function of temperature, however, differs for grains of various sizes and chemical compositions. Within Fundamental rock-magnetism often single grains are analyzed using high-end techniques, so far the obtained information about the grains is only suitable for 2D interpretations. Here we set out to bridge the gap by; non-destructively asses the full magnetic vector of many individual grains within a 'bulk ' sample. This is done by *Micromagnetic Tomography*. Firstly, the distribution and volume of the remanence carrying grains in the sample must be assessed; this is done using a MicroCT scanner capable of detecting grains >1 micron. Secondly, the magnetic stray field perpendicular to the surface of a thin sample is measured using a high-resolution Scanning SQUID Microscope. A mathematical inversion of these measurements yields the isolated direction and magnitude of the magnetic moment of individual grains in the sample. As the measured strength of the magnetic field decreases with the third power as function of distance to the exerting grain (as a result of decay in three dimensions), the magnetization of grains in the top 25 micrometers of the sample can be assessed reliably.

1 Introduction

1.1 Problem statement

The Earth's magnetic field has a pivotal role in the Earth Sciences: its applications range from tectonic reconstructions, dating sections, to the study of the deep Earth. Apparent polar wander can be used to study plate tectonics, describing the movement of the continents relative to the Earth's magnetic pole; magnetostratigraphic, using the polarity of the Earth's magnetic field as a dating tool. Paleomagnetism provides the only window to the deep Earth together with Seismology.

Furthermore, The Earth's magnetic field protects us against harmful cosmic and solar radiation. Understanding the behavior of the Earth's magnetic field on various time scales is therefore important. Capturing reversals of the Earth's magnetic poles, excursions and short lived features is crucial to better understand the past states of the geomagnetic field.

Earth materials are generally magnetized by the Earth's magnetic field as they form. Sediments store magnetization due to magnetic minerals. The magnetic minerals in a sediment will preferably align with the direction of field when the sediment is formed, resulting in a depositional remanent magnetization (DRM). Igneous rocks i.e. lavas, store the magnetization when the rock is cooled from above the Curie temperature, resulting in a thermal remanent magnetization (TRM). The signal of the past state of the Earth's magnetic field can be recovered from reliable recorders, i.e. igneous rocks. Obtaining the full vector from rocks, however, is often not easy; especially obtaining information on the variations in intensity of the field is a challenging task.

Currently, methods to derive paleomagnetic directions and intensities rely on measurements of bulk samples (typically ~10 cc). The measured magnetization is the sum of the magnetization of all the different grains in a sample. The processes of recording and storing magnetizations, however, differ for grains of various grain sizes and chemical compositions. The magnetic carriers in sediments are often quite homogenously distributed; lavas, however, consist of assemblages of grains wildly varying in size, shape, and chemistry. When dealing with lavas, this differing magnetic behavior often hampers paleointensity experiments; while occasionally a reliable paleodirection is obscured (e.g. Coe et al. 2014).

If we would be able to go beyond measurements on the bulk sample, and isolate changes in the magnetic moment per grain during paleomagnetic experiments, opportunities for highly detailed magnetic analyses would be opened. We could unravel the complex bulk magnetic signal and only consider parts of the signal that are stored in grains that are known to be reliable recorders of either paleodirection or intensity. This can lead to a new approach in retrieving paleomagnetic signals from complex mineralogies. It must be noted, however, that the magnetic signal in rocks is a statistical process, and many 'well behaved' grains might need to be assessed individually before a reliable paleodirection and/or intensity can be obtained.

The field of fundamental rock magnetic research currently sees rapid developments, not in the least driven by cutting edge techniques that are often 'borrowed' from material sciences. Our understanding of how the magnetization is recorded within grains and how this magnetization reacts to e.g. temperature changes therefore progresses. Magnetic surface structures i.e. domain states, and interactions can be investigated for example by magnetic force microscopy (MFM) (de Groot et al, 2014 and all references therein). By electron holography (Almeida et al 2015) the vortex state of

remnant structures are studied and variations within grains approaching the Curie temperature. These high end techniques provide better insight in the process of recording the ambient magnetic field (i.e. the geomagnetic field, but also lab fields). These techniques, however, only apply for single grains and do not give insight in the full magnetic vector. Moreover, the sample preparation for all these techniques requires severe processing (cutting, polishing etc) that change the volume (and thereby quite possibly the magnetization) of the grain. Currently the available techniques are therefore not ideal to assess the natural remanent magnetizations stored in Earth's materials.

Here we develop a new technique, *'micromagnetic tomography'*, to isolate the contribution of each magnetic grain in a sample in a nondestructive way, while the grains are still embedded in the bulk sample. This technique opens a wealth of opportunities in fundamental rock-magnetic research. To do so we assess the volume and location of all magnetic particles in a medium with the use of X-ray computed tomography. We measure the magnetization on the surface of the same medium with Scanning SQUID Microscopy. With the known locations of all the magnetic particles and the surface magnetization we are able to isolate the magnetic contribution of each individual grain within the sample, using a computer model. With the use of a computer model we can invert the measured surface magnetization over all the magnetic particles and thereby we can isolate the magnetization per particle.

1.2 Micromagnetic tomography

A typical paleomagnetic rock sample (2.5 cm in diameter, 22 mm long) contains millions of tiny magnetic carriers, often iron-oxides (magnetite (Fe_3O_4) or hematite (Fe_2O_3)). Here we consider their magnetization **M**, and assume that –"far away" from the grains- their magnetic moment **m** is represented by a dipole.

Each magnetization **M** can be represented as a vector spanned by a magnetization in the Cartesian M_x, M_y and M_z directions. The magnetic potential (φ) created by the particle as a function of the vector **r** and dipole moment **m** is given by:

$$\varphi = \frac{(\boldsymbol{m} \cdot \boldsymbol{r})}{4\pi r^3} \qquad (1)$$

Where **r** is the distance vector from the particle to observation point and r is the magnitude of **r**.

The magnetic induction of a dipole at points other than the dipole itself is given by:

$$\boldsymbol{B} = C_m \frac{m}{r^3} [3\,(\boldsymbol{m} \cdot \hat{\boldsymbol{r}})\hat{r} - \boldsymbol{m}] \qquad (2)$$

With $\hat{\boldsymbol{r}} = \frac{1}{r}(x\hat{\boldsymbol{x}} + y\hat{\boldsymbol{y}} + z\hat{\boldsymbol{z}})$, $r = \sqrt{x^2 + y^2 + z^2}$ and $C_m = \frac{\mu_0}{4\pi}$ is a constant. Hence, it is possible to determine the magnetic induction in point P at certain distance from a grain |P-r|, when the magnetic moment **m** of the grain is known. In reverse; if the magnetic induction of a grain is measured in point P and the distance to the grain is known |P-r|; the magnetic moment **m** of the grain can be calculated.

For a paleomagnetic rock sample, the magnetization and magnetic moment of the carriers are unknown, however, the magnetic induction caused by the magnetic grains can be measured. Implying that when the exact locations of the grains and the magnetic induction caused by the grains are known; the magnetic moment **m** can be calculated for each grain.

By X-ray computed tomography (CT imaging) we can assess the exact locations of grains within a sample. CT imaging allows three dimensional characterizations of the grains including size, shape, and location. The surface magnetization flux can be obtained using a Scanning SQUID Microscope. The Scanning SQUID Microscope measures the z component of the magnetic flux (equation 3) at the top surface of the sample.

$$B_z = \frac{\mu}{4\pi}\frac{1}{r^3}\left[3\,\frac{(\boldsymbol{m} \cdot \boldsymbol{r})\boldsymbol{r_z}}{r^2} - m_z\right] \qquad (3)$$

Both data sets can be correlated and used to calculate the magnetization **M** per grain using a computer model. With a computer model the z component of the surface magnetization is inverted over all the grains resulting in a magnetization per grain. The *Inverse model* calculates the magnetization per grain by a Least-Square inversion. The strength of the magnetic induction decays with $\frac{1}{r^3}$, hence, grains "far away" from the measured surface do not contribute to the surface magnetization of a sample, i.e. the magnetic induction due to these grains will not be measured with the Scanning SQUID Microscope. Since there is no magnetization measured, the magnetization for grains far away from the surface is not (correctly) resolved with the Inverse model.

Before performing measurements on real samples; with the MicroCT scanner and Scanning SQUID Microscope, we need to investigate for which sample dimension and dispersion of grains, the magnetization per grain can be reliably calculated with the Inverse model for all the grains within a sample.

We can investigate how well the Inverse model works by using (modeled) *synthetic data* for which the magnetization per grain is known. With a *Forward model* we can prepare synthetic datasets. In the Forward model the exact locations of grains within a modeled sample and the magnetization of all the grain are known. The Forward model calculates the surface magnetization, this is what can be measure (for a real sample) with the Scanning SQUID Microscope; i.e. the Forward model mimics real SSM measurements.

The results from the Forward model; z component of the surface magnetization, can be used as input for the Inverse model. In this way the calculated magnetization by the Inverse model can be compared with the known magnetization. With the two models; Forward and Inverse models, different sample dimensions and dispersions of grains are used to test the stability and accuracy of the Inversion. The optimal sample dimension and dispersion are obtained; for which the inverse model can reliably resolve the magnetization per grain. With this information real samples are made and measured with the MicroCT scanner and Scanning SQUID Microscope.

To have more control over the dispersion of magnetic grains in a sample we are using a synthetic sample for our measurements. Magnetite (Fe_3O_4) grains are evenly distributed in a nonmagnetic matrix material. The sample is magnetized by an anhysteretic remanent magnetization (ARM). The strength of the magnetic induction at the top surface of the sample is a result of all the grains within the sample, since the magnetization of a bulk sample is equal to the sum of the magnetizations of all the grains. The surface magnetization is measured with the Scanning SQUID Microscope and the grains within the synthetic sample are analyzed with a MicroCT scanner. The two data sets are then used as input data for the Inverse model. The Inverse model yields the magnetization for all the grains within our sample. And the Inverse model result; magnetization per grain, underwent several tests to investigate how stable the obtained result is. Here we show that with the technique of micro magnetic tomography; the magnetization of multiple individual grains within a sample can be calculated in a nondestructive way.

2 Methods

2.1 Scanning SQUID Microscopy

In Scanning SQUID Microscopy (SSM) the magnetic surface flux of a sample is measured using a Superconducting QUantum Interference Device (SQUID) (Troeman, 2007; Reith, 2015). In this set-up a SQUID sensor is in near contact with the surface of a magnetic sample, hence the magnetic flux is imaged over a surface grid. The sensor measures the magnetic flux at each point. Here we use the SSM set-up of the Interfaces and Correlated Electron Systems (ICE) group of the University of Twente.

2.1.1 Set up

A direct current SQUID sensor consists of two parallel Josephson junctions (Josephson, 1962) in a circular structure. In this particular setup, the SQUID is extended with a pickup loop (figure 2.1). The pickup loop is made of superconducting material (Niobium) the physical diameter of the pickup loop is 3 µm. The magnetic flux passes through the pickup loop while the remaining elements of the SQUID are magnetically shielded.

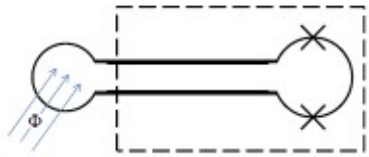

Figure 2.1 Schematic representation of the SQUID sensor extended with a circular pick up loop. The dashes area is magnetically shielded. [Reith, 2015]

This sensor is mounted in the SSM device (figure 2.2). To attain a superconductive state in the sensor, the whole set up, sample and SQUID, is cooled to ~4K by lowering it into a vessel of liquid helium. The position of the sample can be changed with respect to the position of the sensor, its movement is controlled by a *Newport Universal Motion Controller & Driver.* This motion controller can change the x-, y-, and z- position of the sample. The z controller is used to approach the sensor, the x- and y-controllers are used to move the sample across the sensor during a scan. The sensor is kept stationary during a scan and is secured on a cantilever to avoid excess damage to the sensor and/or the sample as a result of irregularities at the sample surface due to the physical contact between the two. The cantilever makes a small angle with the sample surface of approximately 10 degrees (figure 2.3).

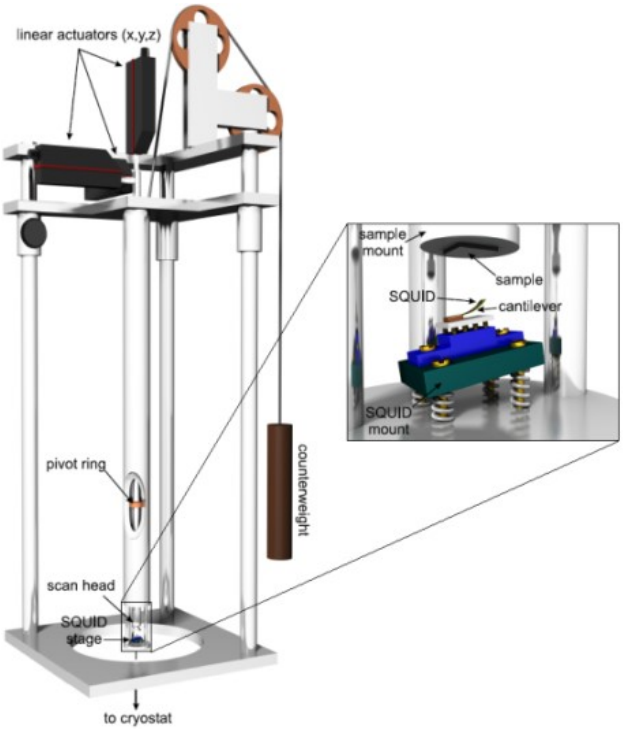

Figure 2.2 Scanning SQUID Microscope, University of Twente. The SQUID sensor is placed on a flexible cantilever. (Troeman, 2007)

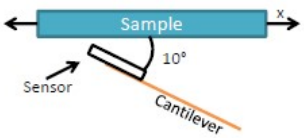

Figure 2.3 Sensor measures the sample under an angle of approximately 10°. (Reith, 2015)

2.1.2 Distance to sample

To measure the flux at the surface of the sample, the tip of the sensor is brought into contact with the sample surface, the sample surface therefore must be smooth and polished. The SQUID measures magnetic flux that penetrates the pickup loop, implying that in our set-up only the z component is measured. Due to the angle of the cantilever, however, some of the in-plane flux components will be measured as well. Due to the flexibility of the cantilever and the angle it makes with the surface, the center of the pickup loop is approximately 2 µm away from the surface. Pushing the sample against the sensor can slightly change the contact angle, hence the distance to the sample.

2.1.3 Effective sensor area

The diameter of the pick-up loop of the SQUID is 3 µm. The effective sensor area is the area of the sample for which the field lines are captures inside the loop at one position. All field lines that are captured inside this loop are measured. Two factors determine the effective area: (1) the angle between sensor and sample, and (2) a phenomenon called flux focusing. The larger the angle between the sensor and the sample, the smaller the effective area. Due to flux focusing the superconducting Niobium pickup loop causes field lines to bend around the pickup loop increasing the effective area (figure 2.4). The effective area of the pickup loop of our sensor is approximately 21 µm^2.

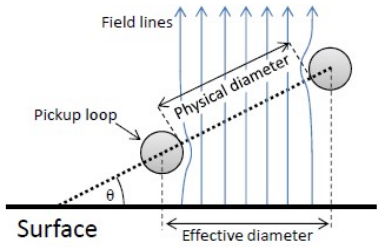

figure 2.4 Representation of the effective sensor area, due to (1) the angle θ between sensor and sample, and (2) flux focusing effect of the superconducting pickup loop. (Reith, 2015)

2.1.4 Noise

The amount of noise in the measurements is due to both internal factors, such as passing the signal between SQUID and the computer, and external factors like passing cars or telecommunication signals.

To lower the noise level caused by external sources, the sample and sensor are shielded by a Niobium tube inside the cryostat. Hence, the Niobium shield becomes superconductive protecting the sample and sensor against ambient magnetic noise. The noise spectrum with the Nb shield is at least one order of magnitude lower than without this shield (figure 2.5). The remaining error caused by the noise level when using the shield is about ± 9 nT.

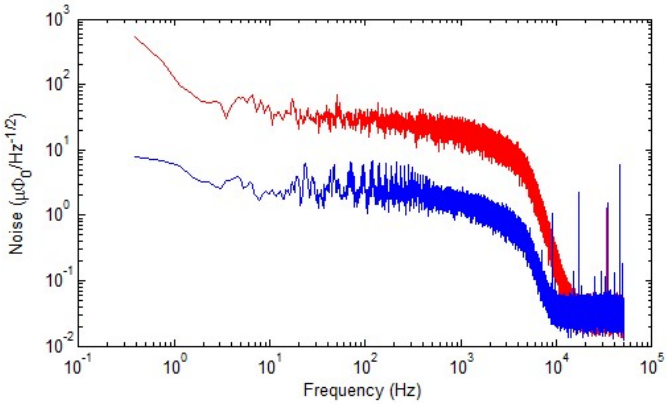

Figure 2.5 Noise spectra of SQUID with (blue) Nb shield and without (red) Nb shield. The sharp drop is due to a low-pass filter (cutoff frequency of 5 kHz) that is built into the system to reduce high-frequency noise.

2.1.5 Scanning specifications

The SSM data is written to a 'BzGrid' matrix of Nx,Ny points. At each grid point the SQUID measures the magnetic flux, which is the integration of the magnetic flux over an area of 21 μm^2 around this point. The spacing between measurement points, i.e. the scan resolution, is set to either 1 or 2 µm. The speed of the sample with respect to the SQUID is set to 30-60 µm/sec. A lower speed increases the scanning time, but improves the signal-to-noise ratio.

The feedback resistance of the SQUID system should be set according to the expected signal strength. For our strong magnetic samples (~1mT), the feedback resistance is set to either 1 of 10 kOhm.

2.2 MicroCT imaging

By X-ray computed tomography (CT imaging) we can assess the exact locations of grains within a sample. CT imaging allows a three dimensional characterization of the attenuation, hence density, distribution. As iron-bearing grains differ in density from the other non-magnetic grains in the sample, the size, shape, and location of the magnetite grains can be obtained. Here we use the MicroCT scanner from the Faculty of Civil Engineering and Geosciences of the Technical University Delft.

2.2.1 X-ray tomography

A tomogram – the data set acquired by tomography – is a three dimensional representation of the variation of structures within a sample, in grayscales. The grayscale values in the tomogram correspond to the apparent X-ray attenuation, giving insight in the density distribution within the sample (Sakellariou et al., 2004). Here we take X-ray images over a 360° rotation with 0.18° intervals, 2000 images in total, and each X-ray image is the average of four exposures.

To locate the iron-bearing minerals in a sample their density needs to be in contrast with the matrix material. The resulting tomogram will include different grayscale values for the grains with respect to the matrix material. Each three dimensional point in the tomogram is called a voxel. The resolution (size of each voxel) depends on the scanning area and density contrast. For small samples (diameter< 1.5 mm) with high-density contrasts the obtained resolution is 0.714 μm^3. The results are stored in DICOM files and interpreted with the visualization program Avizo Fire.

2.2.2 Noise

A phenomenon called beam hardening introduces artifacts in the tomogram. Beam hardening occurs when the X-ray beam scatters back from large density contrasts in the sample, causing a distortion in the signal. To minimize the beam hardening artifacts, a beam hardening correction can be applied to the resulting tomogram (Feldkamp et al., 1984) (Ketcham and Hanna, 2014).

2.3 Summary of the specifications

The z component of the magnetic surface flux is measured by SSM; it yields a matrix of the surface magnetization flux at each scanning point (BzGrid, with Nx times Ny data points). The step size of the grid is either 1 or 2 µm; the effective sensor area is 21 μm^2; and the distance between sample and SQUID is approximately 2 µm. The sample should be polished and should stay in shape at 4 Kelvin.

The volumes, sizes, locations, and a list of voxels per grain is obtained from Micro CT scans; it employs contrasts in attenuation coefficient/density to distinguish grains from the matrix material. To obtain a high resolution only a small area with diameter <1.5 mm can be scanned at once, and the attenuation/density contrasts should be as large as possible.

3 Computational models

For a sample with magnetic carriers (figure 3.1), the z component of the surface magnetization can be measured with the SSM. The magnetization at each grid point is a result of the magnetic moments of all the grains within the sample, equation 3. The exact locations of all the grains within the sample can be obtained by CT imaging. Hence, the only unknown in equation 3 is the magnetic moment **m.** With the use of a computer model, the z component of the surface magnetization can be inverted over all the grains resulting in the magnetic moment per grain. This computer model is called the *Inverse model.*

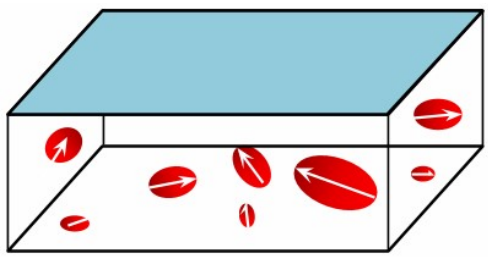

Figure 3.1 Sample with magnetic carriers; grains(red volumes). The grains are magnetized represented by the magnetic moment per grain (white arrow). The z component of the surface magnetization (blue) can be measured with the Scanning SQUID Microscope.

Inverse model: Known: **r** , BzGrid Calculates: **m**

$$B_z = \frac{\mu}{4\pi}\frac{1}{r^3}\left[3\,\frac{(\boldsymbol{m}\cdot\boldsymbol{r})\boldsymbol{r_z}}{r^2} - m_z\right] \qquad (3)$$

Before preparing a sample and performing any measurements on real samples, the equipment specifications e.g. SSM step size and noise levels, as well as the adequacy of the Inverse model must be tested.

We can test our Inversion model with the use of modeled test data. Meaning that we prepare a data set with *known locations of grains* and *known magnetizations* described by the magnetic moments **m**. Using formula 8, we can calculate the z component of the surface magnetization flux at each grid point, BzGrid. Modeled test data can be made with another computer model; the *Forward model*.

Forward model: Known: **r** , **m** Calculates: BzGrid

The Forward model is used to calculate the z component of the surface magnetization flux due to known magnetic moments and locations of grain. The Forward model therefore mimics the result of the SSM. The results of the Forward model; BzGrid, is used as input for the Inverse model (figure3.2). With the Inverse model the magnetization per grain is calculated. The calculated magnetization with the Inverse model can be compared with the implemented magnetization of the Forward model. If the inversion resolves all the magnetizations correctly the magnetic moments are the same. If there is noise during the measurements, however, the calculated magnetic moments should not necessarily be the same as the implemented moments. Influences of noise on the calculated magnetizations with the Inversion model can be tested with the modeled test data (from the Forward model) by adding different noise contributions to the calculated BzGrid matrix.

Also as a result of the decay in three dimensions the strength of the magnetic field caused by a grain decreases with the third power as function of distance to the exerting grain. This implies that grains “far away” from the surface do not contribute to the (measured) surface magnetization. To investigate the thickness of the sample that can be used; i.e. how far grains are allowed to be from the surface to still contribute to the surface magnetization, can be obtained with a combination of Forward and Inverse model. Different sample dimensions and dispersions of grains are used to test the calculated magnetizations obtained with the Inversion. The optimal sample dimension and dispersion are obtained; for which the Inverse model can reliably resolve the magnetization per grain. With this information real samples can be prepared and measured with the MircoCT scanner and Scanning SQUID Microscope.

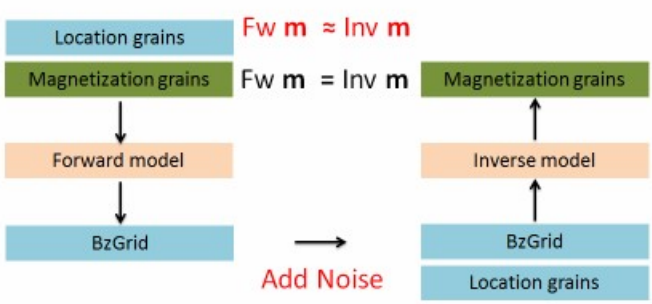

Figure 3.2 Forward & Inverse model. When no noise is added to the BzGrid matrix from the Forward model the magnetic moments for Forward and Inverse model are the same (black). If a noise contribution is added the inverse magnetic moments are an approximation of the implemented magnetic moments.

3.1 Model set up

In both models, Forward and Inverse model, we consider a box with magnetic particles; p= 1 to Npart, for which the location in the sample is known; Coord(Npart, 3). The z component of the surface magnetization is stored in a matrix of Nx by Ny points; BzGrid(i,j) with steps of i= 1, Nx and j= 1,Ny, and step size delta. The distance vector **r** is the difference between the particle coordinate and the grid point location this can be computed for each particle and each grid point. The magnetization in stored as a vector, Magn(NPart,3). The scan height is the distance between sensor and sample surface, generally 2 µm. Both models are written in Fortran90 and the program text can be found in the Appendix.

3.1.1 Forward model

For the forward model, both the magnetization per particle Magn(NPart,3) and the location of the particle within the sample Coord(Npart, 3) are known. With equation 3 the z component of the magnetic flux generated by each particle can be calculated; the magnetic surface contribution is then obtained using the location of the particle and hence the distance to the surface. For each grid point the z component of the magnetic surface contribution for all particles is summed and stored in the matrix BzGrid. The Forward model therefore mimics the result of the Scanning SQUID Microscope, and adheres to the same data format as the SSM’s output data.

3.1.2 Inverse model

The Inverse model uses the z component of the magnetic flux at the surface for each grid point BzGrid(i,j) together with the location of all the particles Coord(Npart, 3) to calculate the

magnetization per particle Magn(NPart,3). This is done using a Least Squares inversion.

The z component of the magnetic flux measured at each grid point BzGrid(i,j), for i= 1,Nx and j= 1,Ny, should be equal to the sum of the magnetic flux calculated for all the particles over all grid points, equation 4.

$$\sum_p B_z\big(\boldsymbol{m}(p)\big) = B_z Grid(i,j) \qquad (4)$$

With the use of a Least-Squares inversion scheme we can solve the magnetic moment per particle. For a least squares inversion the sum of the squares of the residuals i.e. difference between measurements and theoretical value, should be minimum (see box).

Least Squares

Sum of the squared residuals is minimum.

$$S = \sum_{i=1}^{n} r_1^2 \quad , \quad r_i = y_i - f(x_i, \beta)$$

$$\frac{\partial S}{\partial \beta_j} = 2 \sum_i r_i \frac{\partial r_i}{\partial \beta_j} = 0, \; j = 1, \ldots, m$$

The best estimate for the magnetic moment **m**, is found by taking the derivative of the sum of the squared difference with respect to the magnetization and set this to be equal to zero, equation 5.

$$E = \sum_{i,j} || \sum_p B_z\big(\boldsymbol{m}(p)\big) - B_z Grid(i,j)||^2 = min \qquad (5)$$

$\frac{\partial}{\partial m_\beta(q)} E = 0$ with $\beta = 1,2,3$ and q= $1, \ldots, N_{Part}$

Minimizing the derivative of the sum leads to a matrix vector multiplication, equation 6.

$$L\boldsymbol{m}_\alpha(p) = \boldsymbol{b} \qquad (6)$$

Where only the magnetic moment **m** is unknown. Which leads to the inversion equation(7).

$$\boldsymbol{m}_\alpha(p) = L^{-1}\boldsymbol{b} \qquad (7)$$

A detailed derivation for the matrix L and vector **b** can be found in the Appendix. Both matrix L and vector **b** are assembled in the Inverse model; this is done in two separate loops. The inversion calculates the magnetic moment **m** per grain for which the difference between the data and the theoretical value is minimal.

3.1.3 Modeling the grains

Within the Forward and Inverse model we loop over the particles in the sample, these are the grains, the volume and shape of the grains is taken into account in the models. The MicroCT scanner represents the grains as groups of voxels; large grains consist of up to 80000 voxels. Looping over all the voxels in a grain is computationally strenuous; we therefore need to simplify the representation of the grains by grouping the voxels in to larger cuboids; as the models loop over all the cuboids for each grain, it is convenient to have as few cuboids as possible while keeping the volume and shape unchanged. With a routine in 'Mathematica' the voxels are regrouped; in the *voxel-to-cuboid* program neighboring voxels are stepwise regrouped into a larger cuboids, starting with the largest cuboid that fits the (remaining) voxels until none are left (figure 3.3). From approximately 80000 voxels we go down to only 800 cuboids per grain without setting constraints on the volume and/or shape. The program text can be found in the Appendix. The cuboids are assumed to be homogeneously magnetized, and all cuboids belonging to one grain have the same magnetization.

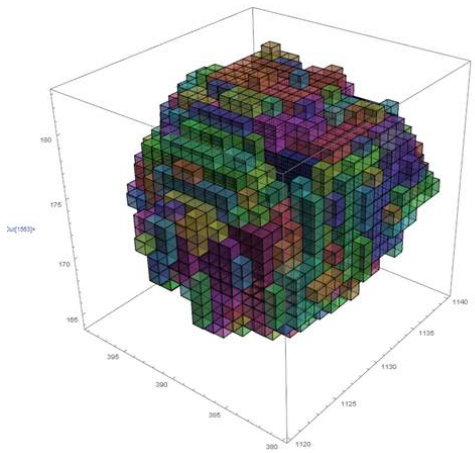

Figure 3.3 One single grain analyzed by the CT scanner. The cubes are the voxels resulting from the CT scanner. These voxels are regrouped into larger cuboids, with a length, width and height. The inner cuboid is the largest, smaller cuboids that fit the remaining voxels are created, visualized by the different colors.

3.1.4 Modeling the sensor

The pick-up loop of the SQUID sensor is circular, with effective area of 21 μm^2. For programming reasons we adopt a rectangular sensor with the same area, resulting in a sensor in the x-y plane with sides of 4.58 μm. For each grid point BzGrid(i,j), the contributions of each particle in the sample, and therefore all cuboids, is integrated over the sensor area.

3.2 Testing the inversion

We start with a model study using the Forward and Inverse models with a modeled synthetic data set of realistic magnetizations and realistic sized grains. The grains in the synthetic data set have diameters of 5-30 µm. The implemented magnetizations for the Forward model are in the order of 1250-5770 A/m. The specifications of the SSM and MicroCT scanner are used, including a grid resolution of 1 µm and a noise level of ± 9 nT. The purpose of this study is to obtain the dimension –and dispersion– of the sample for which we are able to resolve the magnetic moment per grain with the Inverse model, when only the surface magnetization flux (BzGrid) and the exact locations of all the grains are known. This gives information about the samples that can be used in this type of experiments, the dimensions and the dispersion of magnetic grains. How well the inversion works, i.e. solves the magnetization for the grains correctly, can be studied by comparing the calculated magnetization vector **M** -Inverse model result- with the implemented magnetization vector **M** ,input FW model.

The Forward model is used to generate the z component of the magnetic flux at the surface for each grid point; BzGrid(i,j), with a grid spacing of 1 µm. Due to the noise level of the measuring equipment; CT scanner, SSM, factors of noise are included in this model study. This is done by adding a noise related contribution to the BzGrid matrix that is generated by the Forward model. The added noise has a Gaussian distribution. The new BzGrid (including noise) is used as input for the inversion. The calculated magnetizations per grain can be compared with the implemented magnetizations. Different sample dimensions and dispersions of grains (and noise levels) are tested (table 3.1) to find the ideal sample dimension and dispersion of grains for which the magnetizations of all the grains within the sample can be solved with the Inverse model within a ten percent error range.

Model	hsample [µm]	Volume [m^3]	Dispersion [grains/m^3]	Number of grains
Model1	60	2E-12	5.00E+12	10
Model2	60	2E-12	1.00E+13	20
Model3	120	4E-12	5.00E+12	20

Table 3.1 The different sample dimensions and dispersions of grains that are tested. The height of the sample, hsample, is changed to change the dimension. The x and y dimensions are kept constant, 100 by 100 µm.

The implemented magnetizations for the Forward model are in the order of 1250-5770 A/m with an angle with the z axis of 13-52°. The tested noise levels are ± 5, 10, 25 nT.

4 Results

4.1 Testing the inversion

The adequacy of the Inverse model is tested using a synthetic data set for which the implemented magnetization of the grains are known. The synthetic data set is generated with the Forward model. The obtained magnetization with the Inverse model can be compared with the implemented magnetization of the Forward model.

The magnetizations obtained with the Inverse model for the models with a sample height of 50 µm and noise levels of: ± 5, 10, 25 nT, are for all grains within 0.07% of the implemented magnetization. The angles with the z axis for the inverse results are correctly solved within 0.3%.

For the model with a sample height of 120 µm and a noise level of ± 5 and ±10 nT, the inverse magnetizations are solved within 0.8% deviation. The angles for a model with a noise level of ± 5 nT differ 0.0-1.5% from the implemented magnetization angles. The model with noise levels of ± 10 and ±25 nT result in higher angle differences; up to a deviation of 17% (table 4.1). A difference in calculated angle higher than 5% only occurs for grains with a depth below the surface > 68 µm and a noise level of 25 nT. The obtained magnetizations with the inverse model are all very stable, differences in the calculated magnitude of the magnetizations are at maximum 1.82% when a noise of 25 nT is present.

For a noise level of ± 9 nT (SSM specifications) a sample with a thickness of 120 µm and dispersion of 5E12 grains/m^3 can safely be used, for this sample all the grains will be correctly inverted resulting in a magnetization with a magnitude deviating < 1% from the true magnitude. For a higher dispersion 10E12 grains/m^3 a sample height of 60 µm can safely be used. Deviations of only 0.07% from true magnitudes are captured; possibly even thicker samples can be used with the higher dispersion of grains.

Now that the Inverse model in validated and the dispersion and sample height that can be used safely is known; dispersion of 10E12 grains/m^3 and sample height of 60 µm, we can prepare real samples and measure them with the MicroCT scanner and Scanning SQUID Microscope.

Grain	Center depth [µm]	Diameter [µm]	Volume [µm³]	Magnetization [A/m]	Angle θ [°]	Noise 10 M%	Noise 10 θ%	Noise 25 M%	Noise 25 θ%
1	12	14.5	1522.4	1944.1	-51.9	0.00%	0.00%	0.00%	0.00%
2	15	12.8	811.9	3552.3	15.7	0.00%	0.00%	0.00%	-0.01%
3	20	28.1	4835.0	2702.3	-42.3	0.00%	0.00%	0.00%	0.00%
4	25	6.8	267.8	2617.3	36.6	-0.01%	0.02%	0.01%	0.06%
5	28	11.9	704.4	2303.4	-25.7	0.00%	-0.02%	0.01%	0.01%
6	32	23.0	2385.3	5228.8	17.0	0.00%	-0.01%	-0.01%	0.01%
7	37	13.6	1629.9	1250.0	36.9	0.02%	0.06%	0.01%	-0.04%
8	42	23.0	2385.3	3534.3	14.6	0.00%	-0.04%	-0.01%	-0.02%
9	45	17.9	1795.1	5135.4	-13.2	0.01%	0.01%	0.01%	-0.02%
10	50	12.8	811.9	5769.2	-20.6	0.01%	-0.14%	0.10%	-0.07%
11	56	6.8	267.8	5385.2	42.0	-0.20%	-0.17%	1.57%	0.13%
12	61	23.0	2385.3	5023.5	16.4	-0.02%	0.01%	-0.06%	0.00%
13	68	12.8	811.9	2835.5	45.1	0.61%	-0.08%	-0.35%	5.42%
14	76	28.1	4835.0	5228.8	17.0	-0.03%	-0.05%	0.10%	0.43%
15	80	13.6	1629.9	2617.3	36.6	0.15%	0.41%	-0.16%	-0.80%
16	85	17.9	1795.1	2100.0	-48.2	0.58%	-0.35%	1.59%	2.54%
17	89	6.8	267.8	5769.2	-20.6	-0.65%	-12.23%	1.68%	9.64%
18	93	11.9	704.4	2617.3	36.6	0.76%	3.72%	1.82%	-16.88%
19	97	14.5	1522.4	3720.1	23.2	0.40%	1.73%	-1.11%	0.15%
20	102	28.1	4835.0	1250.0	36.9	0.15%	-1.12%	-0.30%	0.92%

Table 4.1. The inverse model results per grain for model3; a sample thickness of 120 µm, and 5000 grains/mm³. The magnitude of the magnetization vector for the forward model is given in A/m, also the angle of the implemented magnetization; this is the angle with the z axis. The results of the inverse model are displayed as deviation from the implemented magnetizations, for a model with a noise of ± 10 and ±25 nT.

4.2 Sample

Synthetic samples are used to obtain the correct sample dimension and dispersion of grains. There are several restrictions for the sample since it should be scanned by both machines, CT scanner and Scanning SQUID Microscope. For the Scanning SQUID Microscope the surface of the sample must be as smooth as possible and the sample should be plan parallel. For the CT scanner a small sample (diameter<1.5 mm) is needed to obtain a high scanning resolution. Also a high density contrast between the magnetic carriers and matrix material is needed.

4.2.1 Sample preparation

For the magnetic carriers in the synthetic sample magnetite grains (Fe_3O_4) are used (Hartstra, 1982). The magnetite grains are crushed and sieved to get grains with diameters in the range of 5-10 µm. To lower magnetic interaction the sieving is done in a sonic bath. Sieves with different mesh sizes are used, starting with the largest mesh; 50, 20, 10 and 5 µm sieves are used. Residual grains are crushed and sieved again. The fraction between 5-10 µm is used for the synthetic sample. Both sieving and crushing is done in alcohol, this prevents the grains from oxidizing. With these grains, we made samples; synthetic samples. The size of the magnetic (synthetic) sample is only a small cylinder with a diameter of 1 mm and a height of 50 µm. This small cylinder is the sample that is measured with the CT scanner, with SSM only the top surface is measured. For measuring and transport reasons the magnetic sample is embedded in a somewhat larger sample holder that can be used in both systems. In this way no shape changes can occur when scanning the sample with different devices and at different temperatures. The sample holder is made of Stycast 2850 FT, this is a two component epoxy resin. Stycast resin is very chemically resistant and is capable to be exposed to cold temperatures (4 K).

Within a rectangular piece of Teflon circular dents are milled with diameters of 3 mm and depths of 2 mm. The holes are filled with the Stycast resin. After the curing cycle of the Stycast the surface is polished. In the Stycast small dents are milled, with a diameter of 1 mm and a depth of 70 µm. These small holes are filled with a mixture of magnetite grains and an epoxy resin; Araldite (table 4.2). This latter resin meets the

following requirements; the density contrast with the magnetite should be as large as possible for the CT scanner. For SSM it should remain in shape at 4 Kelvin. The resin should be chemically quite resistant, since alcohol is used for cleaning and Syton polish for polishing. Of course the magnetic noise of the resin should be zero; non-magnetic resin. And last but not least it should have a low enough viscosity for mixing with magnetite grains.

	Density [g/cm^3]	Density [kg/m^3]	Viscosity [Pa s]
Araldite	1.17	1170	2-5
Calcite	2.710	2710	----
Magnetite	5.175	5175	----
Stycast	2.45	2450	200-250

Table 4.2. Density and viscosity of the resins and grains used for the sample.

Since the magnetite grains have a tendency to cluster together, the grains are premixed with calcite powder. For calcite 10 times the volume of magnetite grains is used. By premixing the grains, calcite covers the magnetite grains and magnetic interaction between magnetite grains is reduced. The right amount of Araldite is added to attain a dispersion of 8000 grains/mm^3. The mix of Araldite, Calcite and Magnetite is poured in the Stycast sample holder.

After the curing cycle of Araldite, the Teflon pieces are polished again. To get a smooth surface and to get rid of surface stress the sample is polished with a silica colloid suspension; Syton polish. After polishing, the samples (figure 4.1) can easily be removed from the Teflon.

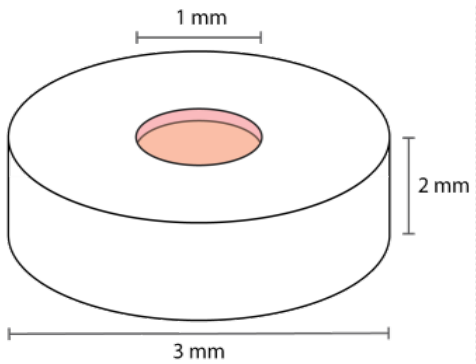

Figure 4.1 Schematic figure of the synthetic sample. Magnetite grains (with araldite and calcite) are located in the inner circle which has a depth of ~70 µm.

4.2.2 Sample magnetization

The samples are imparted with an Anhysteretic Remanent Magnetization (ARM) using an alternating field combined with a DC field. The alternating field has a strength of 300 mT and a DC field of 40 µT is used. The ARM is imparted in the same direction as the alternating field. The ARM is applied perpendicular to the surface. The saturation magnetization of magnetite (Ms) at Room Temperature in field is 480 kA/m, giving a magnetic moment of 90-92 Am^2/kg. Since the sample is magnetized by ARM we expect only 1% of this value (Dunlop and Özdemir 1997).

4.3 MicroCT results

The density contrast within the sample is sufficiently large (table 4.2) to distinguish between magnetite grains and matrix material. The resulting (three dimensional) images successfully visualizes the magnetite grain within the synthetic sample (figure 4.2). The voxel size of 0.714 µm is much smaller than the diameter of the magnetite grains (5-10 µm) used for the synthetic sample. The attenuation coefficient and density of magnetite and calcite are different. Nevertheless the grayscale values do show an overlap (figure 4.3).

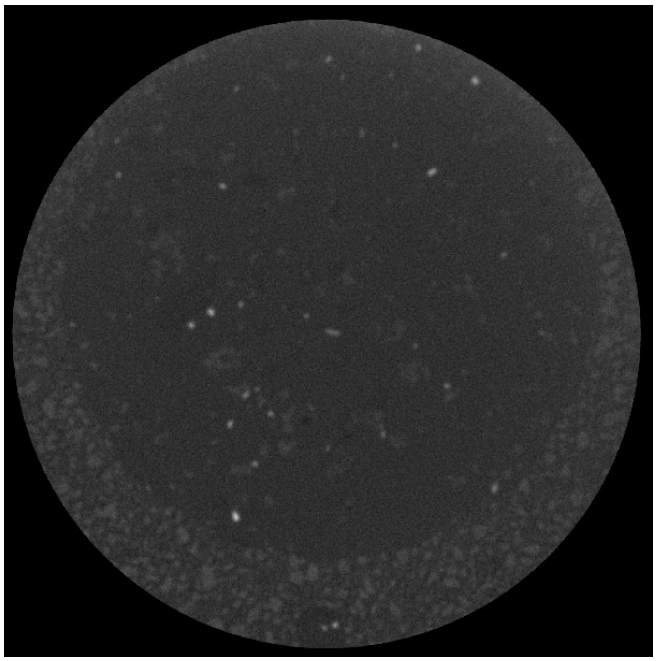

Figure 4.2 Ortho slice of the CT scanner results from the sample. The black inner circle is the location where the magnetite grains are placed, with a diameter of 1 mm. The white spots are the iron oxides - magnetite grains. The correct gray scale values are chosen for magnetite grains.

With the visualization program; Avizo Fire, grains with a volume smaller than 10* voxel volume (10* $(0.714)^3$) are interpreted as calcite, and therefore disregarded. The number of voxels and exact locations are obtained. In total there are 132 magnetite grains in the sample; with diameters ranging from 5-30 µm, this is a result of magnetic interaction of the magnetite grains, and up to 80000 voxels per grain.

4.4 Results SSM Scans

The same sample is scanned multiple times with the Scanning SQUID Microscope, keeping the sample in the cryostat in between measurements. The scanning step size is 1 or 2 µm. Figure 4.4 A and B show the results for scans with step sizes of 1 µm, a feedback resistance of 10 kOhm and a scanning speed of 30 µm/s. These experiments reveal that areas of the surface produce a magnetic field that is outside the measurable range, this results in dark blue and red lines. Due to the strong magnetic signals in the sample the feedback resistance needs to be changed to allow the SSM to pick up the large magnetic fields. Adjusting the feedback resistance to 1 kOhm causes a factor 10 reduction in signal sensitivity. This allows the SSM to measure even the highest magnetic fields emitted by the sample surface (figure 4.4C). The magnetic field strength has a range up to +-10 mT, the color bars are set to +- 100 µT to visualize most of the surface features; displaying the circular shape of the synthetic sample.

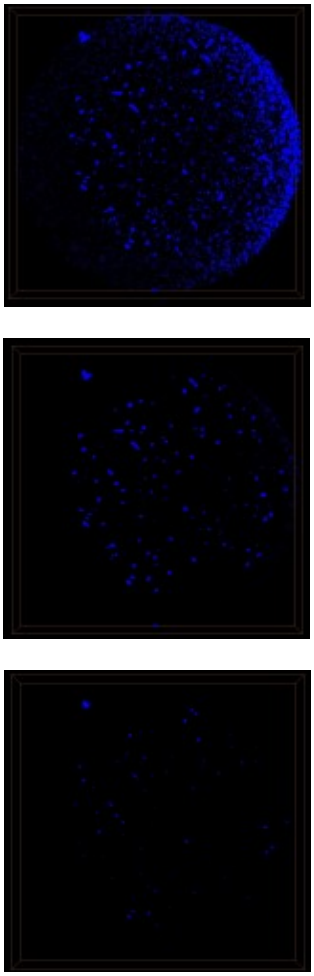

Figure 4.3 Visualization with Avizo Fire. The grayscale values of calcite and magnetite are close. In top figure both magnetite and calcite grains are visible. Also the effect of beam hardening is clearly visible by the outer bright ring on the right side. In the middle figure most of the grains visible are magnetite, the calcite grains that are visible have diameters <5 µm. In bottom figure only the highest densities are selected, the magnetite grains are now smaller indicating the outer rim does not meet the boundary conditions anymore, this changes the volume of the magnetite grains and is not a correct interpretation of the result.

Figure 4.4 Results Scanning SQUID Microscope, measurements on the same sample with differing set-ups. Red spots represent positive magnetic field values, blue negative values, the scale is indicated by the scale bar in micro Tesla. The sample is measured two times with a feedback resistance of 10 kOhm and a step size 1 µm (A&B) revealing the same magnetic structures. The sample is measured with a lower resistance and larger step size (C) indicating identical magnetic structures, all within the measurable range.

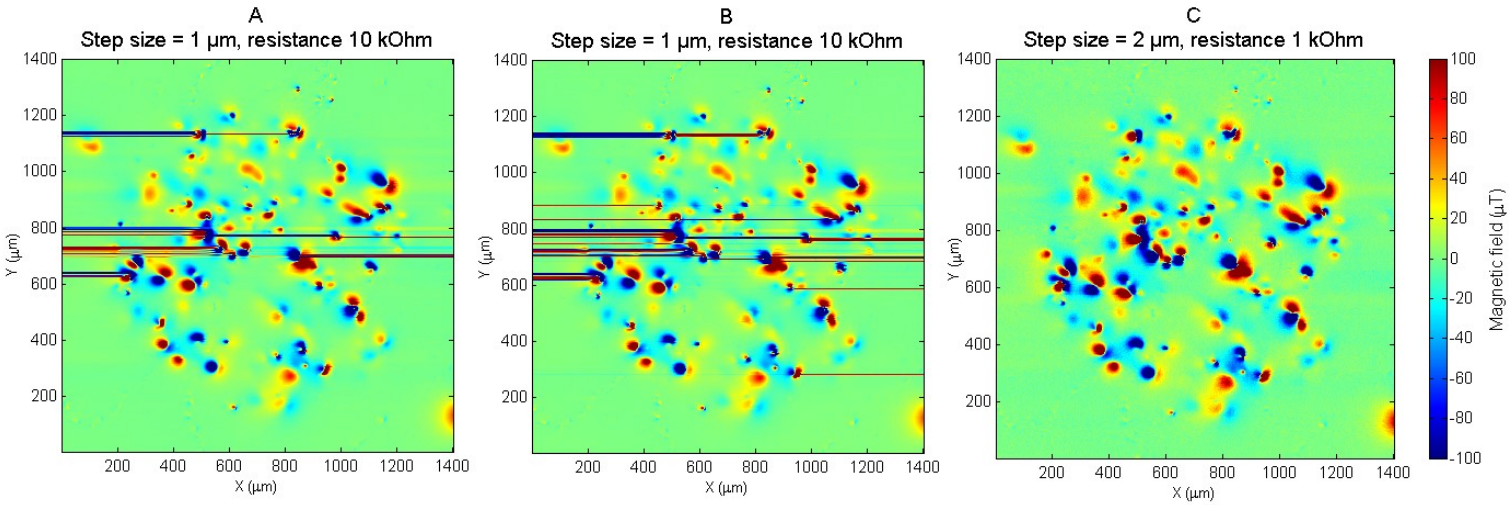

4.5 Mapping

Now that we have the results of both the grains within the sample and the magnetic flux at the surface, we need to correlate the data. The CT scan data gives information about the grains and their location in the sample. This information can be used to map the grains on the SSM result. From equation 3 we know that the grains closets to the surface have the highest contribution to the magnetization measured on the surface. The close surface grains -grains within the first 10 µm – are used to correlate the data sets (figure 4.5). There is a slight offset between the location of the grains and the magnetic surface anomalies; for a voxel size of 0.714 µm the datasets do not align. When assuming a voxel size of 0.85 µm, the grains align better with the magnetic anomalies at the surface. It is, however, not possible to map the grains for the entire sample with the magnetic anomalies at the surface due to apparent distortions. Nevertheless for smaller scan parts the two data sets do align; assuming a voxel size of 0.85 µm. What might have caused this miss match is discussed further below. For now we will only look at a small part of the data for which the grains seem to align with the magnetic surface anomalies. Furthermore, considering only small parts of the sample is computational feasible.

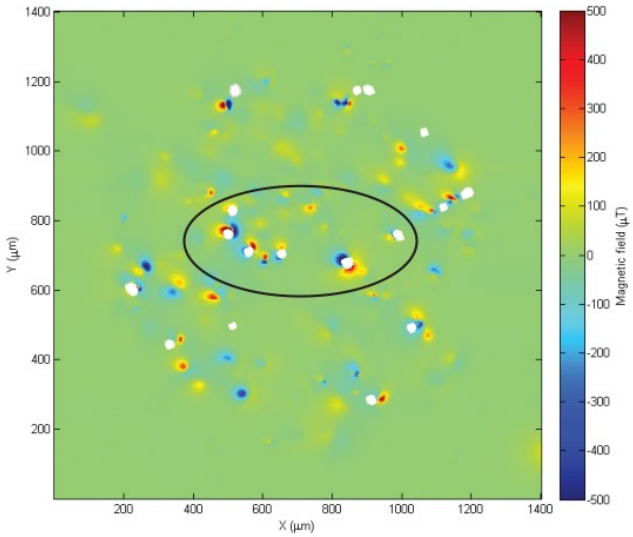

Figure 4.5 Correlating the top surface grains (within first 10 µm) from CT analyses with the SSM measurement results. When the grains in the circle are matched with the magnetic anomalies at the surface, the grains outside the circle do not agree with the magnetic anomalies at the surface.

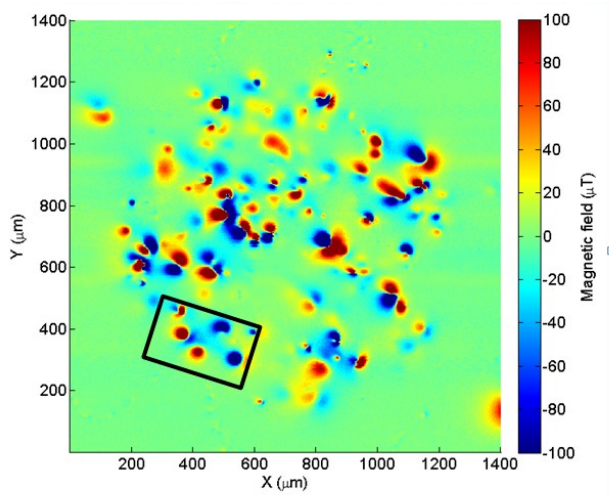

Figure 4.6 Area for which the SSM data is rotated and resampled to match the CT Scanner data is given by the black rectangle.

For small parts of the scan, the grains can be aligned with the magnetic data. The SSM data can be rotated with respect to the grains, figure 4.6, the surface magnetization grid -BzGrid- needs to be resampled to the particle coordinate system. This is done by the use of a resample program written in Mathematica (Appendix) the rotation angle together with a stationary point is implemented. After the rotation and resampling the data is ready for the inversion; figure 4.7.

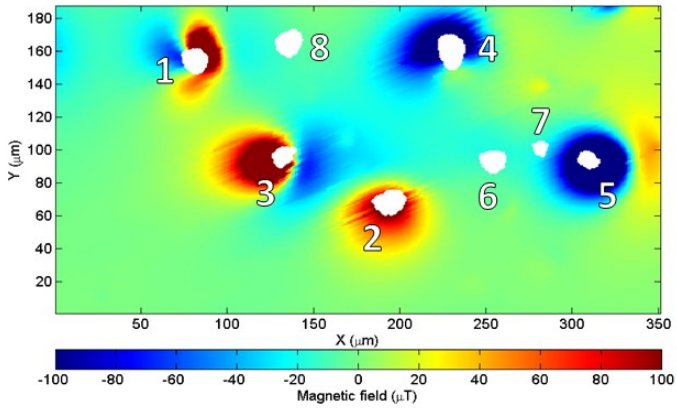

Figure 4.7 Small part of SSM data with mapped grains. The grains are numbered by their depth below the surface; grain 1 is closest to the surface, 4.25 µm, whereas grain 8 is the deepest grain, 44.20 µm. Grains that are closest to the surface have the highest surface contribution, and therefore these grains should map best with the magnetic anomalies.

.

4.6 Inversion result

The Inverse model calculates the magnetic vector for each grain. The resampled magnetic data, together with the locations and sizes of the cuboids are used as input data for the Inverse model. The scanning height, hscan, is set to 2 µm according to the SSM specifications. The results of the inversion are displayed in table 4.3.

The obtained magnetic vectors are in the range 3.4 to 172 kA/m. The magnetic moment per grain is obtained by multiplying with the volume of the grain. The saturation magnetization of Magnetite at room temperature in field is 480 kA/m (Dunlop & Özdemir 1997), grains 3, 5 and 7 show higher results than the 1 percent expected for an ARM; 3.4%, 6.0% and for grain 7 even 36 %.

With the obtained magnetic moment per grain we can run a Forward model to get the magnetization flux at the surface. In this way the scanned data (SSM) can be visually compared to the modeled data, figure 4.8. The overall magnetic structures of the model results excellently agree with the scanned data.

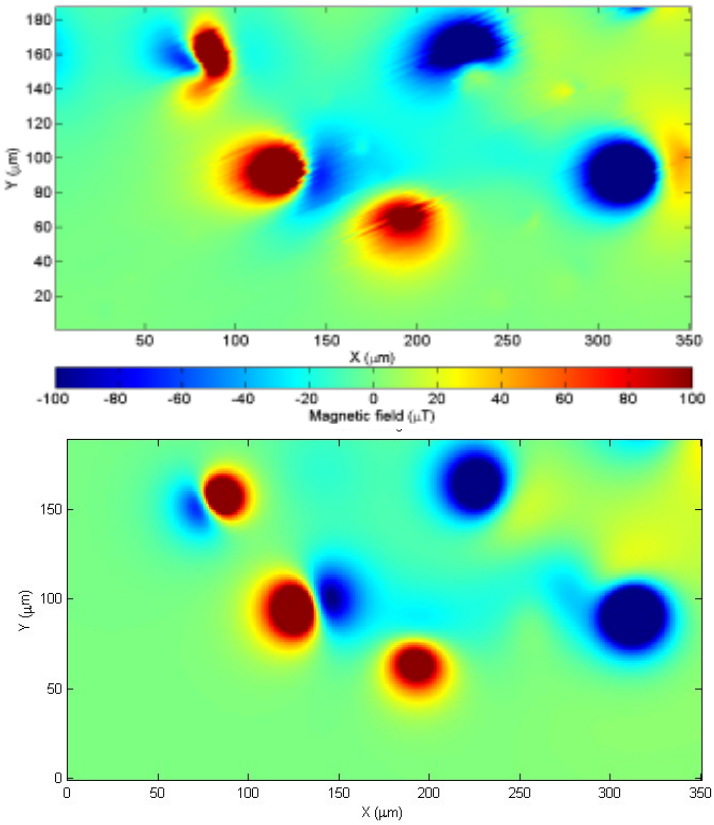

Figure 4.8 Compare measurements (SSM results) in the upper figure to the model results in the lower figure.

Grain	Center [µm]	Diameter [µm]	Volume [µm³]	**M** [A/m]	θ [°]	**m** [Am²]	%Ms
1	11.5	14.5	1522.4	3411.3	-49.9	5.19E-12	0.7%
2	20.8	23.0	2385.3	4225.7	-43.0	1.01E-11	0.9%
3	16.6	12.8	811.9	16129.2	-65.5	1.31E-11	3.4%
4	25.1	28.1	4835.0	3963.8	37.8	1.92E-11	0.8%
5	18.7	11.9	704.4	28637.8	34.1	2.02E-11	6.0%
6	35.3	17.9	1795.1	7047.6	-59.5	1.27E-11	1.5%
7	45.9	6.8	267.8	171932.0	17.8	4.60E-11	35.8%
8	51.0	13.6	1629.9	7401.8	41.4	1.21E-11	1.5%

Table 4.3 Result of the inversion, magnetic vector M in A/m, the angle θ with the z axis, magnetic moment per grain in Am2. The last column is the percent of the Ms (Ms= 480 kAm²/kg).

5 Discussion

The inversion results are promising and emphasize the potential of this new method to bridge the gap between measurements on bulk samples and single grain analyses. The order of magnitude of the magnetizations that are obtained from the inversion are in the expected range: ~1% of the saturation magnetization of magnetite at room temperature, excluding grain 7.

All the grains are resolved with the inversion model: the generated surface magnetization reveals the expected magnetic anomalies; also the in-plane dipolar features for grain 1 and 3 are resolved. The calculated surface magnetization matrix (BzGrid) from the Forward model can be subtracted from the original scanned data. In this way the difference between the real data and modeled data can be visualized, figure 5.1. The differences between scanned data and model data visualize scanning artifacts e.g. scanning lines.

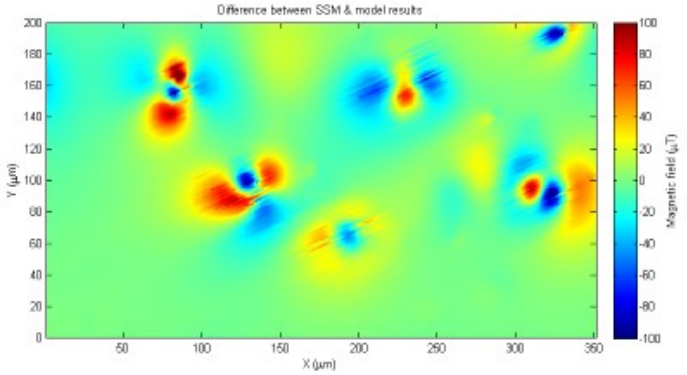

Figure 5.1 Difference between scanning data (SSM) and data from the models. The lines are a scanning effect.

5.1 CT data cut off

The data set obtained with the CT scanner consists of a detailed list of all the voxels for each particle within the sample. The size and shape of these particles are determined by manually selecting the range of grey values that are believed to represent the iron-oxides. It is therefore important to consider the effect on the obtained inversion results when this range of grey values would be varied. By narrowing this range the grains become smaller e.g. the outer rim of the grains does not meet the boundary conditions of the selected range anymore. Hence, the volume of the grains does change quite rapidly when the thresholds are changed. To assess this effect, we assessed what happens if a modeled particle with dimensions of 20 x 20 x 20 µm is interpreted as a particle of only 18x18x18 µm, so if the outer layer of voxels is not taken into account. A combination of Forward and Inverse models can be used to investigate the effect.

In figure 5.2 the magnetic flux generated by a cubic particle (20x20x20 µm) is shown. The squares show the different particle dimensions used for the inversion. The magnetization of the particle is defined as **M**=(800, 0, 2400) [A/m]. With the Forward model the BzGrid of the particle with dimension 20x20x20 µm is calculated. The results for the inversion (table 5.1) with the same particle dimensions show that the magnetization is perfectly resolved. An inversion with a particle for which the outer shell of voxels (voxel size ~1 um) is removed (18x18x18 µm), results in a 36.8% increase of the calculated magnetization for the particle. When removing another shell of voxels, magnetization almost doubles, and is overestimated by 92.4%. The direction of magnetization is very constant for the different particle dimensions. Theta, the angle with the z-axis, varies <1%.

When a particle is interpreted smaller than the real size of the particle, the magnetization obtained by the inversion is an overestimate for that particle. Selecting the proper range of grey values is therefore very important, as the volume of the particle changes rapidly even if only a thin outer layer of the grain is not considered. Nevertheless, for comparative purposes (i.e. when different magnetic states of the same sample are considered) the changes of the magnetization with respect to the original state are of interest. So even if a particle is interpreted to be smaller than the true dimensions of that particle it does not affect relative changes as long as the dimensions of the grains are kept constant throughout the entire experiment.

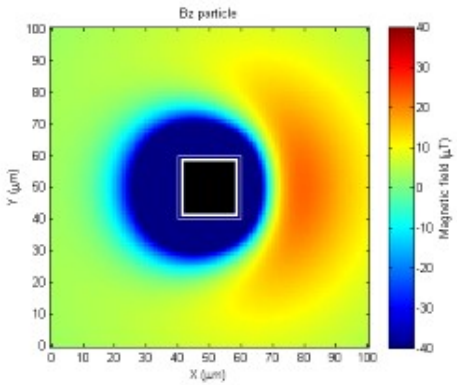

Figure 5.2 Particle of 20x20x20 µm. Outer white square is the original particle, inner whit square a particle with dimensions of 18x18x18 and inner black square shows particle with dimensions of 16x16x16.

	Dim [µm]	Volume [µm³]	M_x [A/m]	M_y [A/m]	M_z [A/m]	M [A/m]	Theta [°]	Overestimate
Forward	20x20x20	8000.0	800.0	0.0	2400.0	2529.8	18.4	
Inverse	20x20x20	8000.0	800.0	0.0	2400.0	2529.8	18.4	0.0%
	18x18x18	5832.0	1094.8	16.9	3283.2	3461.0	18.4	36.8%
	16x16x16	4096.0	1539.0	0.0	4616.9	4866.7	18.4	92.4%

Table 5.1 Results for the magnetization of a grain when the original particle has dimensions of 20x20x20 µm. The Inverse model is ran with the magnetic flux generated by the forward particle. Volume, magnetization in the three directions, magnetization vector M, Theta is the angle with the z axis and a quantification of the overestimate of the magnetization with respect to the original magnetization.

5.2 SSM oversampling

The Scanning SQUID Microscope scans the sample line by line with a speed of 30-60 µm/s. For a scanning resolution of 1 µm the SQUID measures the magnetic flux penetrating the pickup loop each micrometer. The effective area of the pickup loop –the area of the sample that is measured at one position– is 21 µm^2. The sensor therefore measures the magnetic flux over an area (figure 5.3), and is stored at the center of this area in the BzGrid matrix. Each measurement is an average over the effective area. Each grid point, for a grid spacing of 1 micrometer, is measured 21 times by the sensor at the surrounding grid points. The oversampling of the magnetic flux is taken into account in the inversion model. With this oversampling the signal to noise ratio will improve due to averaging over an area.

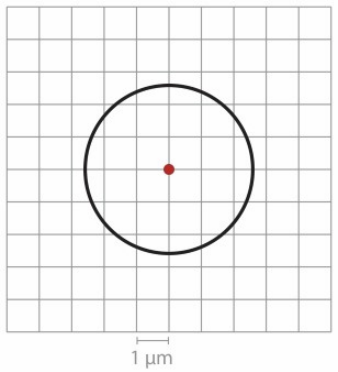

Figure 5.3 Effective area of the SQUID sensor. Grid spacing of 1 µm. A measurement at one grid point (red dot) is a result of the magnetic flux penetrating the SQUID over the area given by the black circle; 21 µm^2.

5.3 Data miss match

The voxel size that results from the MicroCT does not agree with the scanning data obtained with SSM, there is a miss match between the data sets. Even if the voxel size is changed so that the grains better align with the magnetic anomalies, the two data sets still do not form a perfect fit for the entire sample. For small parts of the sample, however, the data sets can be matched with confidence. To assess the influence of possible errors in matching the SSM data onto the MicroCT data, we assessed how the sample moves with respect to the sensor in the SSM setup. In the SSM set up, the sample is moved with respect to the sensor. The sample is moved in the x-y direction, the z component does not change. The sample, however, is placed on a pendulum/swing and the top is kept stationary. The displacement in x- and y-direction will therefore influence the distance to the sample. Due to the small displacement in the z direction, the angle of the cantilever with respect to the sample changes and the distance to the sample is now larger than 2 µm. Due to the change in angle and distance the data can slightly deform at different locations. How the data is deformed can be checked with markers on the surface of the sample. When the exact shape and dimensions of a marker are known, the scale of deformation, and the regions on the sample that are prone to this effect can be determined. Markers that are suitable for this setup are Niobium (Nb) markers. Nb markers are visible both optically and with the SQUID since the Nb will become superconducting at 4K. Unfortunately the process of placing markers at the sample surface did not work for our synthetic samples. For lava samples the process of placing markers is more promising. With lava samples (or other suitable ground for markers) the deformation due to the scanning can be visualized. When the change in distance and the angle is known, we can correct for this change and the grains should align with the magnetic scanning data. For now we will only focus on a small area (350 by 180 micrometers) for which the grains do align with the magnetic scanning data. For only small areas the change in angle and/or distance between sample and sensor is minimal, therefore we can reliably invert the signal for small areas.

5.4 Scan height

With the Scanning SQUID Microscope samples are scanned with the center of the pickup loop approximately 2 µm above the sample surface, for the Inverse model a scan height of 2

µm is therefore used. The scan height influences the distance between the measured magnetic flux and the location of the grains for which magnetic induction is calculated. The effect of a slight error in the scan height can be tested by considering our modeled cubic particle again. The test particle has dimensions of 20 x 20 x 20 µm and consists of 1000 cuboids which all have dimensions of 2 x 2 x 2 µm. The center of the particle is placed in the middle of a 100 by 100 grid point scan at a depth of 30 µm.

Running forward models with different values for hscan, the scan height above the sample surface, gives insight in how the magnetic flux at the surface will change with increasing scanning distance. As expected, the magnetic surface flux decreases with increasing scanning distance, figure 5.4. Next, the inverse model is used to see how the magnetic moment of the particle reacts on a scan height that is different than the one used for the forward model. For example, if the Forward model scans the sample at 1 µm we did the inversion with a scan height of 2 µm. If the sample is scanned at a larger distance with the forward model than is used in the inverse model, the calculated magnetic moment is an underestimation, in the case of the test sample ~9%, table 5.2. The other way around, if the forward model scans the sample closer than is implemented for the inverse model, the calculated magnetic moment is an overestimation, here ~9%.

The resulted magnetic moments for our area of interest; real data, are obtained with an Inverse model using the best estimate of the scan height; hscan= 2 µm. So we assume that the pickup loop of the SQUID sensor is 2 µm away from the surface. If the sensor is pushed against the sample, the angle changes slightly and the distance between senor and sample decreases. This would imply that the calculated magnetic moments are underestimations of the real magnetic moments (table 5.3). For the grains with good defined magnetic anomalies at the surface, i.e. grains 1-5, inverting the data with a scan height of 0 µm and 1 µm indeed yield an underestimation (respectively ~22% and 11%) when comparing the calculated moments with the results for an inversion with a scan height of 2µm. For these grains an Inversion with a scan height of 3 µm yields an overestimation of ~12% compared with the results for hscan= 2µm. The angle with the z axis does not significantly change for the four different scan heights, only ~3%.

The deeper grains without a prominent surface magnetic anomaly, however, give over- and under- estimates the other way around. Inverting the data with a scan height of 0 µm and 1 µm yields overestimations, while intuitively an underestimation is expected. The angle with respect to the z axis changes significantly, 10-43%, compared to the angle of the result with a scan height of 2 micrometers. Deeper grains accommodate the change in magnetization at the surface by changing the angle with the z axis; theta, this explains the counterintuitive change in magnetization.

For grains close to the surface, ~top 13 µm, the results are very stable even when the inverse model is ran with an over- or underestimation for the scan height. For grain further from the surface, with depths > 26 µm, the inverse result obtained is less stable for differing scan heights.

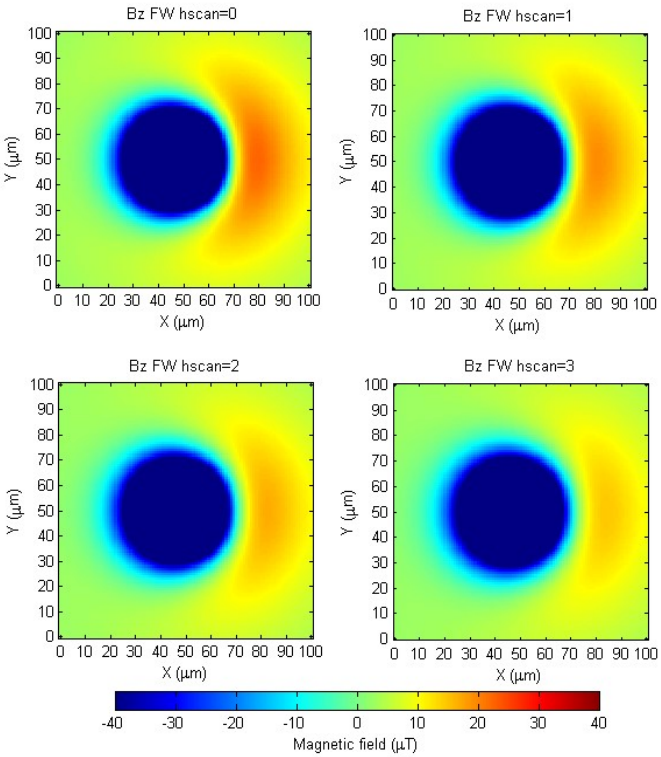

Figure 5.4 Forward models of the sample with a test particle with magnetic moment m=(800 , 0 , 2400). The scan height differs from hscan=0 until hscan=3. The dipolar structure is better defined for models with smaller scan heights, compared to models with higher scan heights. This is visible by the red and blue areas.

Model	hscan [µm]	M_x [A/m]	M_y [A/m]	M_z [A/m]	M [A/m]	Diff
FW	1	800.0	0.0	2400.0	**2529.8**	
Inv	0	728.0	0.0	2184.9	**2303.0**	-9%
	1	800.0	0.0	2400.0	**2529.8**	0%
	2	874.5	0.0	2621.7	**2763.7**	9%

Table 5.2 Influences of the scan height. Using a Forward model with a known magnetization (M_x , M_y , M_z) and a scan height of 1 µm. The inversion is run with differing scan heights. This results in differing magnetizations, and can be compared to the implemented Forward magnetization (Diff).

Grains	hscan=2µm M [A/m]	Theta [°]	hscan=0µm M [A/m]	Diff	Theta [°]	hscan=1µm M [A/m]	Diff	Theta [°]	hscan=3µm M [A/m]	Diff	Theta [°]
1	**3411.3**	-49.9	**2464.4**	-28%	-52.4	**2921.8**	-14%	-51.1	**3932.6**	15%	-48.7
2	**4225.7**	-43.0	**3339.4**	-21%	-43.2	**3771.5**	-11%	-43.1	**4701.7**	11%	-42.8
3	**16129.2**	-65.5	**12424.2**	-23%	-65.7	**14223.6**	-12%	-65.6	**18141.1**	12%	-65.5
4	**3963.8**	37.8	**3267.8**	-18%	36.3	**3609.1**	-9%	37.0	**4332.1**	9%	38.6
5	**28637.8**	34.1	**22610.3**	-21%	37.3	**25502.0**	-11%	35.7	**32040.1**	12%	32.5
6	**7047.6**	-59.5	**8146.4**	16%	-70.7	**7665.8**	9%	-65.5	**6313.9**	-10%	-51.9
7	**171932.0**	17.8	**174080.0**	1%	15.0	**172112.4**	0%	13.6	**174593.4**	2%	25.8
8	**7401.8**	41.4	**10091.3**	36%	59.2	**8566.1**	16%	51.3	**7150.9**	-3%	36.5

Table 5.3 Inverse model results for different scan heights. The obtained magnetization and angle with z axis (Theta) are compared to the inverse model with scan height of 2 µm

5.5 Mapping perturbation

The mapping of the SSM data onto the MicroCT data is done by placing the grains closest to the surface (with the highest contributions to the magnetization on the surface) onto the most prominent magnetic anomalies in the SSM data. To assess the sensitivity of the obtained inversion to small misalignments we perturb the mapping. With eight more (inversion)model runs the 'original' location can be shifted with 2 µm in both positive and negative x- and y directions. Results of this perturbation are shown in figure 5.5. The results look all very similar. For the new models again a plot of the difference between scanned data results and model data results can be made; figure 5.6.

The magnetic moments resulting from the inversion are displayed in table 5.4. The original scan is given in the middle. For the eight perturbation models the obtained magnetic moments is compared with the magnetic moment for the original mapping. For the close surface grains, grain 1-5, the deviations are below 10%. The deeper grains, with a distance to surface>26 µm, grain 6-8, the obtained magnetic moments result in differences larger than 10%. Grain 7 is located close to a large negative magnetic anomaly. This anomaly belongs to grain 5, however, due to the shift of the grains, grain 7 is located onto the anomaly and this field is used for the inversion. This grain therefore does not give reliable results.

Grains 1 and 3 are close to the surface <15 µm and show clear magnetic anomalies in the SSM results. The model runs with a perturbation in x- and y- direction also show these magnetic anomalies. The direction of the magnetization, however, differs. When comparing the model 'xmin-yplus' (top left) with 'xplus-ymin' (bottom right) grain 1 is resolved better by the xmin-yplus model while grain 3 is better solved by the other model. This is also viable in the 'difference' figures, where the difference between the BzGrid from the SSM and the BzGrid from the model is visualized (figure 5.6). Especially grain 1 and 3 are differently resolved for the models. The grains with a more vertical magnetization are less prone to mapping perturbation and hence a difference in magnetic vector.

Another way of comparing the model results with the scanned data is to make a histogram of the difference matrix. When the model results resolve the data perfectly, the difference matrix will be filled with zero's. In all our nine cases there is a slight offset, figure 5.7. The width of the distribution indicates how well the surface magnetization is resolved. The nine histograms, however, all show a more or less evenly wide distribution.

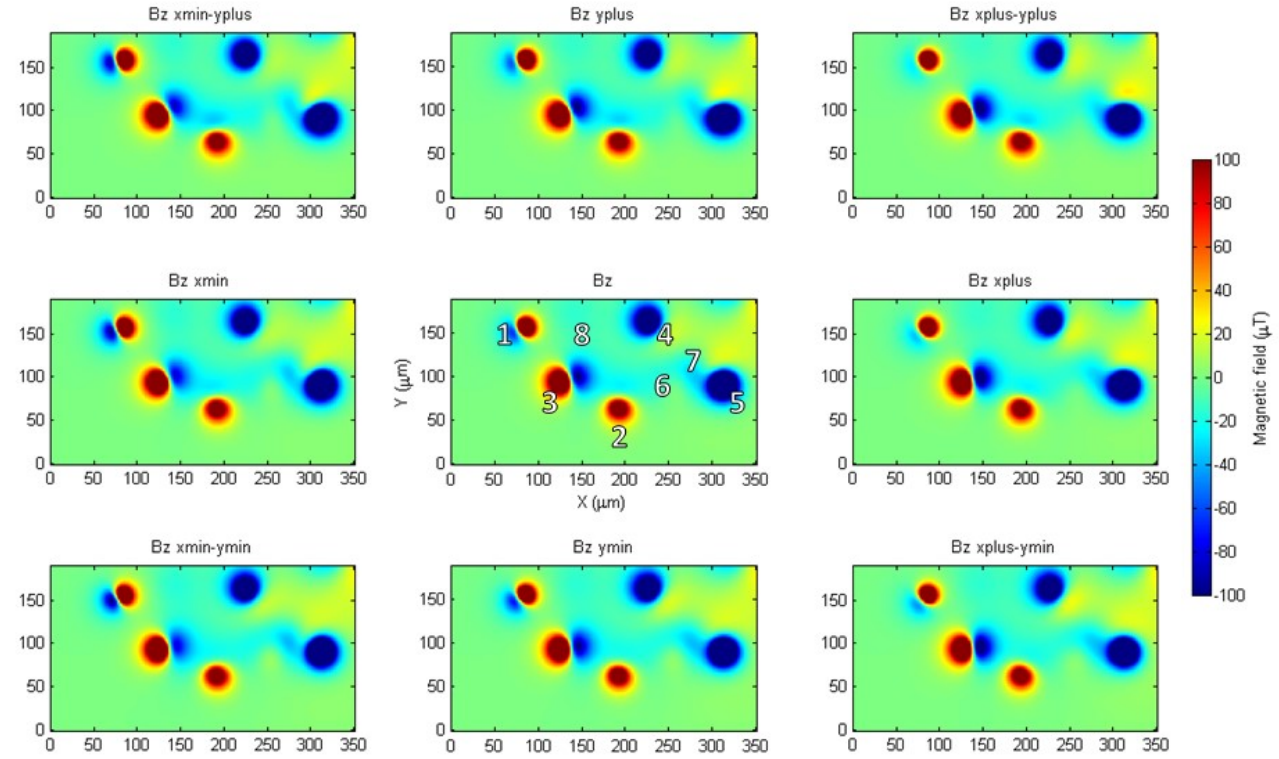

Figure 5.5 Results of a mapping perturbation for SSM and CT data. The grains are shifted with respect to the magnetic anomalies in x-and/or y-directions, with displacements of 2 µm. The 'original' mapping is the middle figure. The scan height is kept constant at 2 µm.

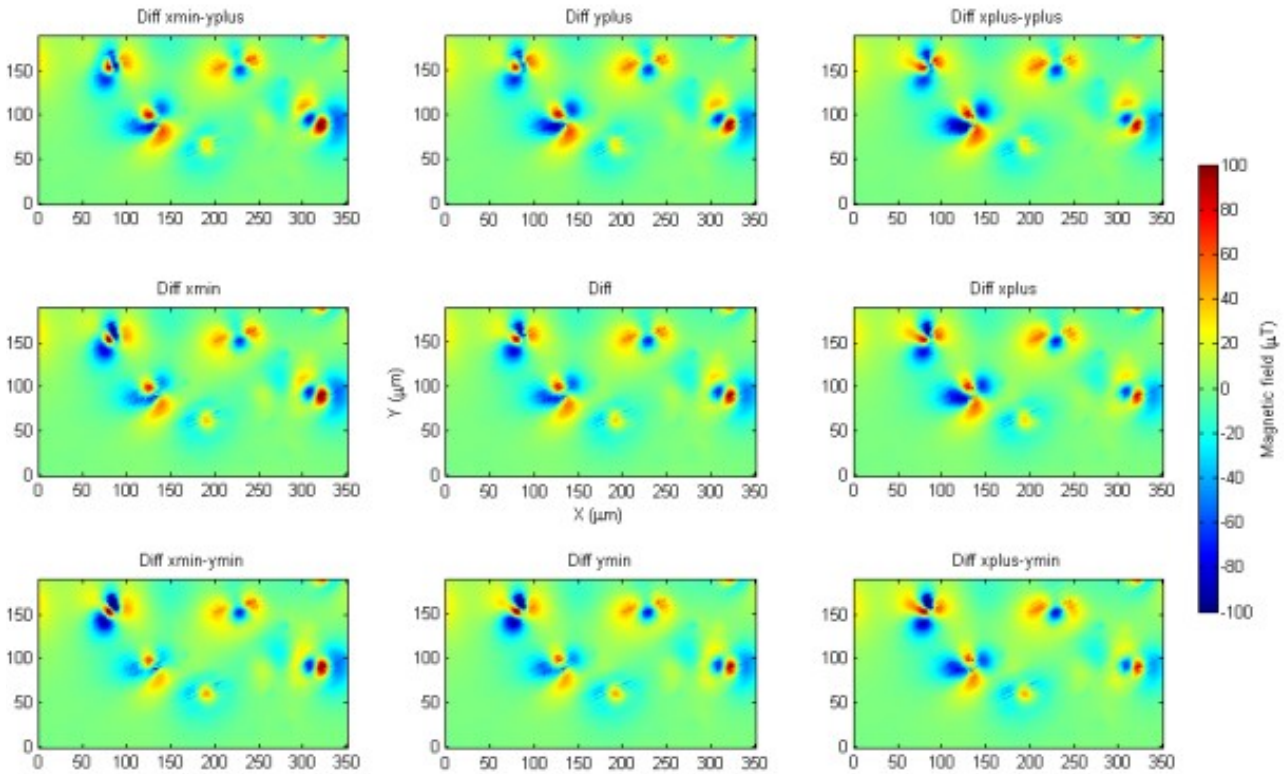

Figure 5.6 Mapping perturbation differences between SSM data and modeled data. Displacement in x-and/or y-directions of 2 µm. The 'original' mapping is the middle figure.

Table 5.4 Mapping perturbation results for the obtained magnetizations and angle with the z axis (Theta). The results are compared to the original mapping. Grains for which the deviation with the original mapping is larger than 10% are marked red.

Grain	M [A/m]	Theta [°]	Deviation
1	3677.2	-58.1	7.8%
2	4447.4	-50.6	5.2%
3	15479.4	-62.0	-4.0%
4	3793.4	26.3	-4.3%
5	29905.9	47.7	4.4%
6	8416.6	-67.6	19.4%
7	194365.9	3.9	13.0%
8	8619.7	49.3	16.5%

Grain	M [A/m]	Theta [°]	Deviation
1	3424.1	-45.2	0.4%
2	4386.4	-50.6	3.8%
3	15793.0	-67.5	-2.1%
4	3887.0	32.7	-1.9%
5	29427.4	42.5	2.8%
6	6404.9	-70.1	-9.1%
7	161460.9	4.7	-6.1%
8	7408.2	45.7	0.1%

Grain	M [A/m]	Theta [°]	Deviation
1	3110.8	-28.7	-8.8%
2	4364.5	-51.8	3.3%
3	15794.0	-72.8	-2.1%
4	3970.3	38.4	0.2%
5	29271.5	39.0	2.2%
6	4483.7	-77.1	-36.4%
7	128019.1	7.2	-25.5%
8	6549.7	47.3	-11.5%

Grain	M [A/m]	Theta [°]	Deviation
1	3610.5	-61.4	5.8%
2	4269.4	-42.8	1.0%
3	15666.5	-59.3	-2.9%
4	3875.1	32.6	-2.2%
5	29288.1	41.3	2.3%
6	9034.8	-59.3	28.2%
7	205618.4	15.9	19.6%
8	8458.5	46.1	14.3%

Grain	M [A/m]	Theta [°]
1	3411.3	-49.9
2	4225.7	-43.0
3	16129.2	-65.5
4	3963.8	37.8
5	28637.8	34.1
6	7047.6	-59.5
7	171932.0	17.8
8	7401.8	41.4

Grain	M [A/m]	Theta [°]	Deviation
1	3134.0	-36.2	-8.1%
2	4227.7	-44.9	0.0%
3	16244.4	-71.4	0.7%
4	4036.9	42.6	1.8%
5	28387.7	28.8	-0.9%
6	5191.8	-62.7	-26.3%
7	136745.3	19.8	-20.5%
8	6832.5	43.8	-7.7%

Grain	M [A/m]	Theta [°]	Deviation
1	3428.9	-64.7	0.5%
2	4079.8	-34.1	-3.5%
3	15773.5	-57.3	-2.2%
4	3991.0	39.5	0.7%
5	28827.3	36.2	0.7%
6	10148.5	-55.0	44.0%
7	221822.6	25.6	29.0%
8	8902.0	46.7	20.3%

Grain	M [A/m]	Theta [°]	Deviation
1	3298.4	-54.6	-3.3%
2	4058.7	-34.8	-4.0%
3	16348.8	-64.2	1.4%
4	4067.1	43.6	2.6%
5	28036.7	26.6	-2.1%
6	8367.6	-54.9	18.7%
7	189265.7	28.8	10.1%
8	7801.5	40.6	5.4%

Grain	M [A/m]	Theta [°]	Deviation
1	3085.8	-43.6	-9.5%
2	4086.8	-37.8	-3.3%
3	16546.7	-70.5	2.6%
4	4122.2	47.5	4.0%
5	27695.4	18.3	-3.3%
6	6781.8	-57.8	-3.8%
7	154982.0	32.6	-9.9%
8	7413.9	42.9	0.2%

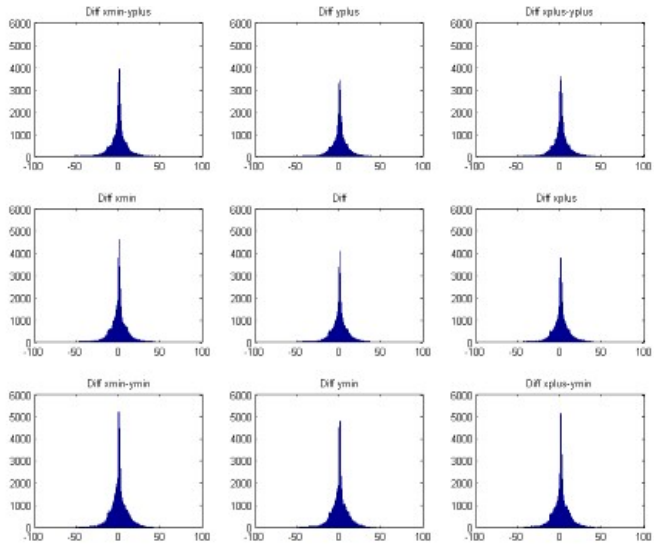

Figure 5.7 Distribution of the difference between real data (SSM) and the results from the Inverse model.

5.5.1 Surface features

The surface features that are visible in the SSM results (figure 5.8) are not recreated by the models. These features can be an effect of the angle of the cantilever and the scanning direction. The sample is moved with respect to the SQUID sensor. The sample is scanned line by line, moving the sample in the x direction. After each line the sample is moved in the y direction to scan the next line. The SSM result shows lines due to the scanning direction. Also the visible magnetic anomalies show blurring off to the left side. This can be explained by the sensor being under an angle. Since the SQUID sensor is assumed to be parallel to the surface these surface features are not created by the models.

5.6 Model assumptions

5.6.1 Homogeneously magnetized

The particles are assumed to be homogeneously magnetized, i.e. the magnetic moment is represented by a dipole. This is valid for Single Domain grains, but only an approximation for Multi Domain grains. MD grains deeper within the sample, 'far away' from the scanner, will behave like a dipole. For grains close to the surface the structures within the grain can contribute to the surface magnetization flux measured with the Scanning SQUID Microscope. The SSM result for our area of interest do not directly show structures within the grain for the closest grain ~4 µm from the surface. Grain number 1, however, is not resolved correctly by the models. The outcome of the perturbation models show that the magnetization for this grain can be solves in multiple ways, whereas none of the magnetic surface fluxes from these models explain the SSM data. For this grain it is possible that the dipole assumption is violated and that the grain is therefore not correctly resolved. The inversion result for close surface grains (~upper 3 µm) might not be correct due to the dipole assumption, and should not be considered for experiments.

5.6.2 SQUID sensor

Both Forward and Inverse models consider the effective area of the SQUID sensor. The effective area of the circular pickup loop is approximated to be 21 μm^2, this can vary for different sensors, scan height and angle with the sample. For the models, Forward and Inverse, the sensor is assumed to be a square with an area of 21 μm^2. Thus the same area is used although the shape of the sensor is approximated by a square instead of a circle. This can have an influence on the grains close to the surface since there the magnetic flux is directly measured with the SQUID sensor. For grain deeper within the sample, however, this assumption is valid. Since the sensor scans over an area rather than at one point, the measurement is an average over the area. The angle the sensor makes with the sample is not taken into account in the models. Due to the angle the sensor will also pickup some of the in-plane magnetizations. The angle is approximately 10 degrees.

5.7 ARM direction

The Scanning SQUID Microscope measures the magnetic flux in the z direction. The ARM for the sample is imparted perpendicular to the surface, in the z direction. This does not necessarily mean that the individual grains are all magnetized in the z direction, since storing the magnetic signal is a statistical process. The obtained magnetization vectors are either positive or negative and are distributed in two cones around the z axis, table 4.3. The angle with the z axis varies between 17.8°-65.5°.

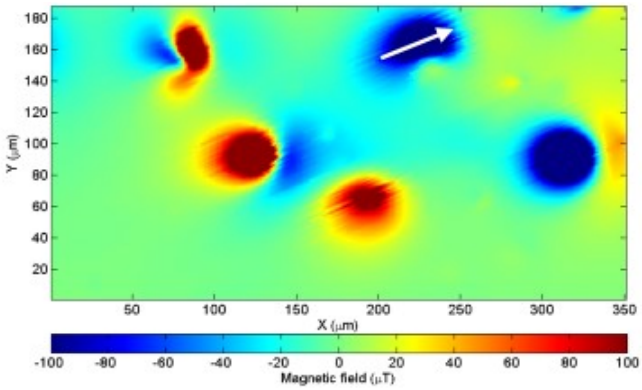

Figure 5.8 SSM result for the area of interest. The lines are a result of the scanning direction, white arrow. On the left side of the anomalies the signal is blurred due to the angle of the cantilever.

5.8 Outlook

Since storing the magnetic signal is a statistical process, many grains might need to be assessed individually before a reliable paleodirection and/or intensity can be obtained. For paleointensity experiments this setup is not ideal since the measurements are performed at 4K, this is below the Verwij transition (for magnetite Tv= 120K). The noise level and resolution of the equipment, however, are sufficient to obtain reliable inversion results. The coupling of MicroCT data and SSM is still a bit tricky, however, the obtained inversion results for the upper grains (<25 µm) show stable results. The mapping can be simplified by the use of Niobium markers on the sample surface. With the use of markers, the exact position with respect to the grain can be obtained; also markers will give insight in the scan height. We are interested in relative changes for the magnetization for different grains within the sample after a demagnetization step, e.g. AF demag. Using markers the position of the grains can easily be assessed, and relative changes be can investigated for single grains within a bulk sample. MicroCT results of a lava sample indicates a dispersion of 70,000-80,000 Grains/mm^3, magnetite grains with diameters ranging from 1- 50 µm. Grain smaller than 1 µm, however, are not detected due to the MicroCT resolution.

6 Conclusion

With Micromagnetic Tomography the full magnetic vector of many individual grains within a bulk sample are obtained in a nondestructive way. A mathematical inversion of the surface magnetization over the exact locations of the grains yields a reliable magnetization for grains in the top 25 micrometers of a sample. Grains close to the surface, i.e. within 25 µm are very stable for mapping and scan height perturbations. The obtained magnetization vectors and the angle of the magnetization with respect to the ARM direction are within 10% variations. Deeper grains >45 micrometers, are prone to mapping and scan height perturbations. This new method bridges the gap between measurements on bulk samples and single grain analyses, creating great potential for fundamental rock magnetism.

Acknowledgement

First of all I would like to thank my advisor, Lennart de Groot. Lennart, without you my research project would not only be non-existent, I would not be the researcher I am today if it wasn't for you. Thank you for all our discussions, your opinion on the matter and the urge to never give up.

I would like to thank Karl Fabian from NGU in Trondheim for the mathematical and modeling support. Your help made it possible to run and of course create the computer models. I am very gratefully that you are always available for a Skype meeting and always in for a new trick to overcome the next 'problems'.

This interdisciplinary research project would not have been possible without the help of Pim Reith, Ankur Rastogi, André Timmermans and Hans Hilgenkamp from the MESA+ institute for nanotechnology of the University of Twente and Auke Barnhoorn from the CITG of Delft University of Technology. I am grateful for their help, support, and enthusiasm while working on this project!

References

Almeida, T.P., Muxworthy, A.R., Kovács, A., Williams, W., Dunin-Borkowski, R.E., 2015. Visualisation of high temperature magnetisation states in magnetite grains using off-axis electron holography. Journal of Physics: Conference Series, 644 (1), 012027

Coe, R.S., Jarboe, N.A., Le Goff, M., Petersen, N., 2014. Demise of the rapid-field-change hypothesis at Steens Mountain: The crucial role of continuous thermal demagnetization. Earth and Planetary Science Letters, 400, p. 302-312.

Dunlop, D.J., Özdemir, Ö, 1997 Rock Magnetism, Fundamentals and frontiers. Cambridge University Press, Cambridge and New York. 573 pp.

de Groot, L.V., Fabian, K., Bakelaar, I.A., Dekkers, M.J., 2014. Magnetic Force Microscopy reveals meta-stable magnetic domain states that prevent reliable absolute palaeointensity experiments. Nature Communications, 5, p. 1-10.

Feldkamp, L. A., Davis, L. C., Kress, J. W., 1984. Practical cone-beam algorithm. Journal Optical Society of America A, 1, 6.

Hartstra, R.L., 1982. Some rockmagnetic parameters for natural iron-titanium oxides, Ph.D. Thesis, Utrecht University.

Josephson, B.D., 1962. Possible new effects in superconductive tunneling. Physics Letters, 1, p. 251-235

Ketcham, R.A., Hanna, R.D., 2014. Beam hardening correction for X-ray computed tomography of heterogeneous natural materials, Computers &Geosciences, 67, p. 49–61

Reith, P., 2015. Imaging Ferromagnetirsm on the Mircometer Scale A Scanning SQUID Microscope Study, MSc Thesis, University of Twente.

Sakellariou, A., Sawkins, T.J., Senden, T.J., Limaye, A., 2004. X-ray tomography for mesoscale physics application. Physica A, 39, p. 152-158.

Troeman, A. G. P., 2007. NanoSQUID magnetometers and high resolution scanning SQUID microscopy, Ph.D. Thesis, University of Twente.